# Plasmoids observed in the near-Earth magnetotail at X ∼ −7 R E

Y. Miyashita, A. Ieda, Y. Kamide, S. Machida, T. Mukai, Y. Saito, K. Liou, C.-I. Meng, G. K Parks, R. W Mcentire, et al.

# Plasmoids observed in the near-Earth magnetotail at $X \sim -7\ R_E$

Y. Miyashita,[1] A. Ieda,[1] Y. Kamide,[1] S. Machida,[2] T. Mukai,[3] Y. Saito,[3] K. Liou,[4] C.-I. Meng,[4] G. K. Parks,[5] R. W. McEntire,[4] N. Nishitani,[1] M. Lester,[6] G. J. Sofko,[7] and J.-P. Villain[8]

Received 13 June 2005; revised 22 August 2005; accepted 22 September 2005; published 16 December 2005.

[1] Recent studies have statistically shown that the magnetic reconnection site at substorm expansion onset is located in the magnetotail at $X \sim -20\ R_E$ on average. For a substorm event that occurred at ~0153 UT on 2 July 1996, however, Geotail observed a series of tailward but slow flows with southward magnetic fields fairly close to the Earth at $(X, Y) \sim (-7, 9)\ R_E$. The flows had enhancements of the total pressure and the total magnetic field as well as bidirectional field-aligned low-energy electrons in their central part. We interpret these as signatures for tailward moving small plasmoids with scales of $\sim 0.5-3\ R_E$. Considering that GOES-8 observed a dipolarization at $(X, Y) \sim (-4, 5)\ R_E$ after the expansion onset, we estimate that the magnetic reconnection occurred between the Geotail and GOES-8 positions. UVI auroral images from Polar and ground magnetic field data show that this substorm, initiated at ~20 hours MLT and ~64° magnetic latitude, was not very intense, and the period examined was not during an intense storm. The southward interplanetary magnetic field (IMF) was not very large, while the large duskward IMF persisted for more than 12 hours before the onset as well as the somewhat large solar wind dynamic pressure. It seems likely that the global ionospheric convection was not very strong. Locally enhanced convection and auroral oval expansion due to the large IMF $B_y$ and the solar wind dynamic pressure might lead to the initiation of the magnetic reconnection much closer to the Earth than usual.

**Citation:** Miyashita, Y., et al. (2005), Plasmoids observed in the near-Earth magnetotail at $X \sim -7\ R_E$, *J. Geophys. Res.*, *110*, A12214, doi:10.1029/2005JA011263.

## 1. Introduction

[2] Magnetic reconnection [e.g., *Baker et al.*, 1996] as well as dipolarization or current disruption [e.g., *Lui*, 1996] in the near-Earth magnetotail plays a crucial role in triggering substorm expansion onsets. It was shown that the magnetic reconnection site, i.e., "near-Earth neutral line (NENL)," at substorm expansion onset is located, on average, at $X \sim -20\ R_E$ or $-20 > X > -30\ R_E$ [e.g., *Baumjohann et al.*, 1989, 1999; *Nagai et al.*, 1998; *Machida et al.*, 1999; *Miyashita et al.*, 2000, 2003]. The location in individual cases, however, depends on the substorm intensity: it tends to be located closer to the Earth in more intense substorms [*Miyashita et al.*, 2004]. The magnetic reconnection site retreats tailward in the late expansion or recovery phase of the substorm [*Forbes et al.*, 1981; *Angelopoulos et al.*, 1996], as predicted by the near-Earth neutral line model [*Hones*, 1976]. Hence the magnetic reconnection and resultant plasmoid can be observed more frequently at larger distances down the tail [*Ieda et al.*, 1998; *Ueno et al.*, 1999]. In rare cases the magnetic reconnection can occur at $X \sim -13\ R_E$ [*Baker et al.*, 1996]. Recently, *Miyashita et al.* [2005] also reported that the magnetic reconnection occurred earthward of $X \sim -8.6\ R_E$, associated with very intense substorms during the 30 October 2003 superstorm.

[3] Plasmoids generated by the magnetic reconnection evolve as they move tailward. Their typical $X$-directional length and duration are, respectively, ~4 $R_E$ and ~1 min at $X \sim -30\ R_E$ and ~10 $R_E$ and ~2 min in the middle and distant tail [*Ieda et al.*, 1998]. Plasmoids are, however, smaller in $X$ size and shorter in duration in the near-Earth tail. *Slavin et al.* [2003, 2005] examined flux ropes at $-10 > X > -30\ R_E$ and traveling compression regions (TCRs) at

[1]Solar-Terrestrial Environment Laboratory, Nagoya University, Toyokawa, Aichi, Japan.
[2]Department of Geophysics, Kyoto University, Kyoto, Japan.
[3]Institute of Space and Astronautical Science, Japan Aerospace Exploration Agency, Sagamihara, Kanagawa, Japan.
[4]Johns Hopkins University Applied Physics Laboratory, Laurel, Maryland, USA.
[5]Space Sciences Laboratory, University of California, Berkeley, Berkeley, California, USA.
[6]Department of Physics and Astronomy, University of Leicester, Leicester, UK.
[7]Institute of Space and Atmospheric Studies, University of Saskatchewan, Saskatoon, Saskatchewan, Canada.
[8]Laboratoire de Physique et Chimie de l'Environnement, Centre National de la Recherche Scientifique, Orléans, France.


0148-0227/05/2005JA011263

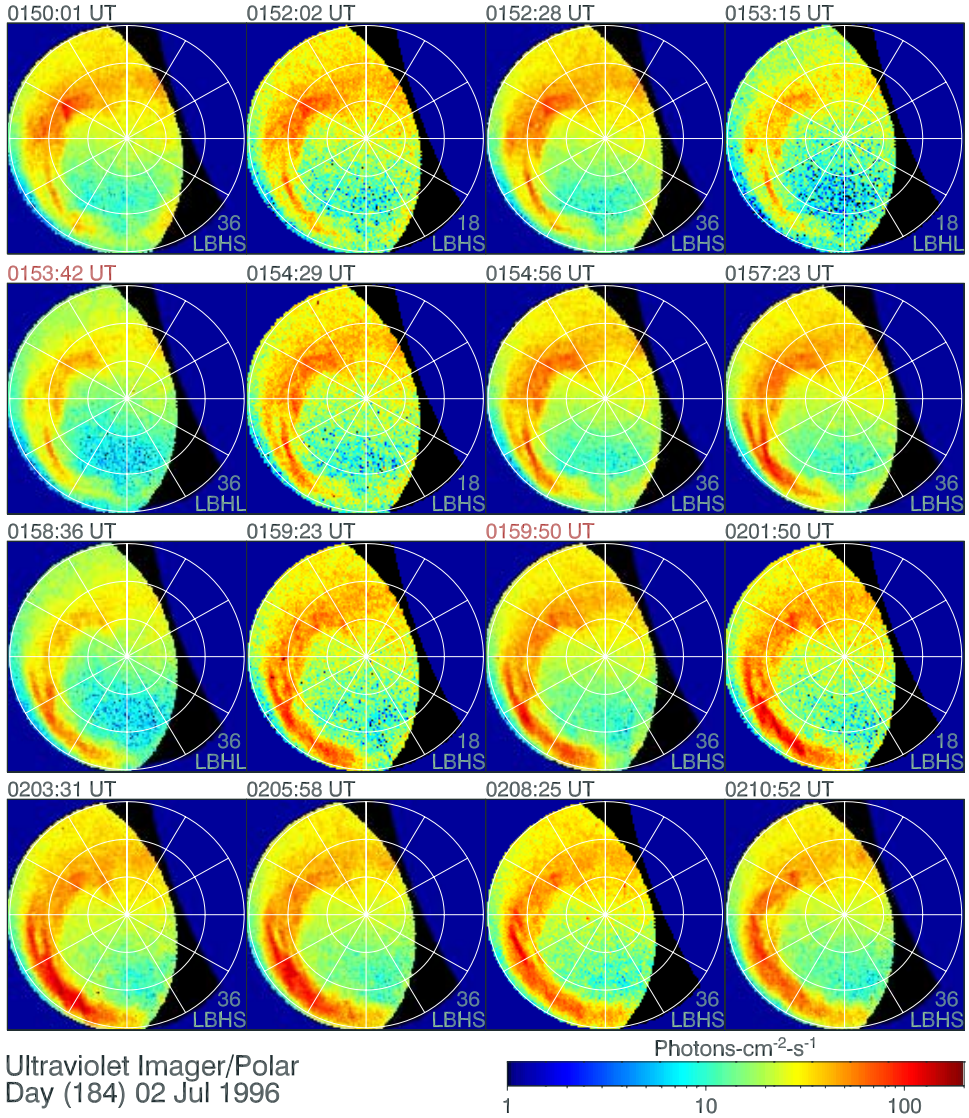


**Figure 1.** Selected auroral images from Polar UVI from 0150 to 0211 UT on 2 July 1996, showing the substorm expansion onset at 0153:42 UT ±18 s (labeled 0153:42 UT) and the intensification at 0159:50 UT ±18 s (labeled 0159:50 UT). The magnetic midnight and dusk are plotted to the bottom and left, respectively. The contours of AACGM magnetic latitudes are drawn from 90° with a decrement of 10°. The time indicated at the top of each panel is the center of data integration period in universal time.

$-11 > X > -19\ R_E$, which were related to plasmoids and moved tailward and earthward. They found that the typical size and duration are ~1–4 $R_E$ and ~30 s, respectively. *Ieda et al.* [2001] also reported small plasmoids in the near-Earth tail, which were closely correlated with auroral brightenings.

[4] The purpose of the present paper is to demonstrate that the magnetic reconnection ("NENL" formation) can occur even earthward of $X \sim -7\ R_E$. In a substorm event that occurred at ~0153 UT on 2 July 1996, the Geotail spacecraft observed several tailward flows with southward magnetic fields at $X \sim -7\ R_E$, which we interpret as small plasmoids, suggesting that the magnetic reconnection occurred earthward of this location. It is much closer to the Earth than the average location and than even locations for superstorms. This substorm was not very intense, and the period examined was not during an intense storm. Geotail was located in the close vicinity of the magnetic field lines mapped to the auroral onset region [*Frank et al.*, 2001]. In the present paper, we examine this substorm event in closer detail and discuss the associated plasmoids.

## 2. Observations

### 2.1. Aurora and Geomagnetic Field

[5] Figure 1 shows selected auroral images from the Polar ultraviolet imager (UVI) [*Torr et al.*, 1995] in the altitude-adjusted corrected geomagnetic (AACGM) coordinates [*Baker and Wing*, 1989]. The auroral breakup or the substorm expansion was initiated at ~20 hours MLT and ~64° magnetic latitude at 0153:42 UT ±18 s (labeled 0153:42 UT), although at higher latitudes, an enhanced auroral arc extended from ~19 hours MLT and ~68° to ~22 hours MLT and ~64°, persisting from ~2140 UT of

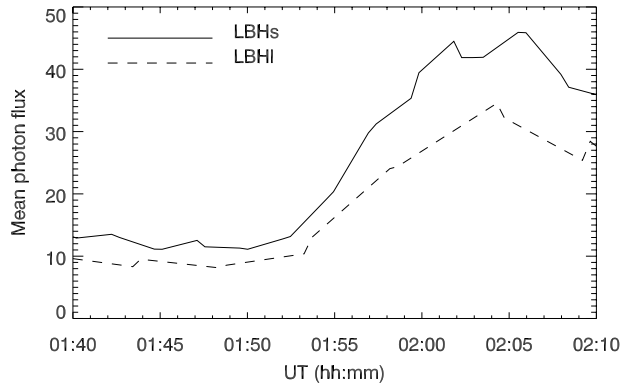


**Figure 2.** Mean photon fluxes in photons $cm^{-2}$ $s^{-1}$ from the LBH-short (solid line) and LBH-long (dashed line) filters in a region of 62–65° magnetic latitude and 19.5–20.5 hours MLT from 0140 to 0210 UT.

the previous day. The onset time is also determined from Figure 2, which shows mean photon fluxes from the LBH-short and LBH-long filters around the onset region, i.e., in a region of 62–65° magnetic latitude and 19.5–20.5 hours MLT. The mean photon fluxes started to increase at ~0153 UT. The onset latitude of this substorm was a few degrees lower than typical latitudes of ~66° [e.g., *Craven and Frank*, 1991; *Liou et al.*, 2001].

[6] The auroral bulge then expanded in the poleward and azimuthal directions, but the poleward expansion was not very significant immediately after the onset. The auroral bulge started to develop further at 0159:50 UT ±18 s (labeled 0159:50 UT) at 20–21 hours MLT and ~65°. Such stepwise development of the auroral bulge is not uncommon in some substorms [e.g., *Kadokura et al.*, 2002]. The auroral bulge subsided after ~0208 UT. It extended from ~18 to ~0 hours MLT and from ~61° to ~68° at the maximum stage. Note that the equatorward auroral boundary shifted to the very low latitude of ~61°.

[7] We also examined the corresponding geomagnetic field data to confirm the substorm onset signatures. Figure 3a shows the north-south magnetic field at selected high-latitude ground stations from 0050 to 0250 UT on 2 July 1996. The time resolution is 1 min for Poste-de-la-Baleine (PBQ) and Narsarsuaq (NAQ) and 5 s for the CANOPUS stations [*Rostoker et al.*, 1995]. These stations were located in the vicinity of the region of the substorm auroral activity examined in the present study. Clear negative perturbations associated with the westward auroral electrojet were observed at 0151 UT at Gillam (GILL) and PBQ at ~19 and 20.5 hours MLT and ~66°, reaching maximum magnitudes of ~160 nT and ~240 nT, respectively.

[8] Figure 3b shows the north-south magnetic field obtained with 1 min resolution at low- and middle-latitude ground stations. Positive bays started at stations at ~20–21 hours MLT at 0153 UT, simultaneously with the auroral onset, but they did not grow very much immediately after the onset. They grew larger at most of the stations only after 0157 UT, reaching a maximum value of ~20 nT at St. Johns (STJ). Note that the enhancements of the northward geomagnetic field at 0134 UT were due to the small enhancement of the solar wind dynamic pressure at this time. Figure 3c shows Pi2 pulsations at a low-latitude station, Hermanus (HER). Onset times of the Pi2 pulsations are identified as 0146 and 0152 UT. The latter probably corresponds to the auroral onset at 0153 UT. These geomagnetic signatures for the substorm onset and intensification are consistent with the auroral signatures. According to the auroral and geomagnetic observations, the substorm examined here was not very intense, although the onset latitude was a few degrees lower than the typical latitudes.

[9] The second panel from the bottom in Figure 4 shows the 1 min resolution *SYM-H* index, which is equivalent to the *Dst* index. The *SYM-H* index is seen to decrease to ~−30 nT around the substorm expansion onset, indicating that the substorm examined here did not occur during an intense storm.

### 2.2. Solar Wind

[10] Figure 4 shows the 80–90 s resolution solar wind parameters and the 1 min resolution interplanetary magnetic field (IMF) obtained from the Wind solar wind experiment (SWE) and magnetic fields investigation (MFI), respectively. The data are shifted by a propagation time from the Wind position of GSM $X \sim 211$ $R_E$ to the dayside magnetopause, roughly estimated to be ~62 min. The solar wind number density remained large, ~20 $cm^{-3}$, leading to a somewhat enhanced dynamic pressure of ~4–5 nPa, after their jumps at ~1320 UT on 1 July 1996. The IMF also jumped at ~1400 UT on 1 July 1996, resulting primarily from the enhancement of the duskward component. The southward IMF was not very large, ~−5 nT and ~−10 nT at most, before the substorm expansion onset, while the duskward component was consistently large, ~10 nT. The IMF was directed nearly duskward, and there were no particular changes of the solar wind and the IMF at the substorm expansion onset, although there were small fluctuations.

### 2.3. Near-Earth Magnetotail

[11] We describe the Geotail observations in detail in this subsection. Figure 5 shows the locations of Geotail and GOES-8 in the GSM *X-Y* plane during the period of 0050–0250 UT on 2 July 1996. Geotail was located in the premidnight sector of the near-Earth magnetotail at ($X$, $Y$) ~ (−7, 9) $R_E$ ($R \sim 12$ $R_E$). According to the geomagnetic field models T89 (T96) by *Tsyganenko* [1989, 1995], the footprint of Geotail at the substorm onset was at 67.2° (67.2°) AACGM latitude and 20.3 (19.9) hours MLT, ~3° poleward of the auroral onset region. Here the input parameters used for the models were hourly values of the solar wind dynamic pressure of 3.47 nPa, the IMF $B_y$ of 11.6 nT, and the IMF $B_z$ of −3.4 nT, the *Dst* index of −19 nT, and the *Kp* index of 3−.

[12] Figure 6 shows the ion moments and the magnetic field obtained from the low-energy particle experiment (LEP) [*Mukai et al.*, 1994] and the magnetic field experiment (MGF) [*Kokubun et al.*, 1994] on board Geotail with 12 and 3 s resolution, respectively, during the 2 hour period of 0050–0250 UT on 2 July 1996 in GSM coordinates. Geotail was in the northern plasma sheet throughout the period, except for the equatorial crossings during 0152–0156 UT and the movement away from the central plasma

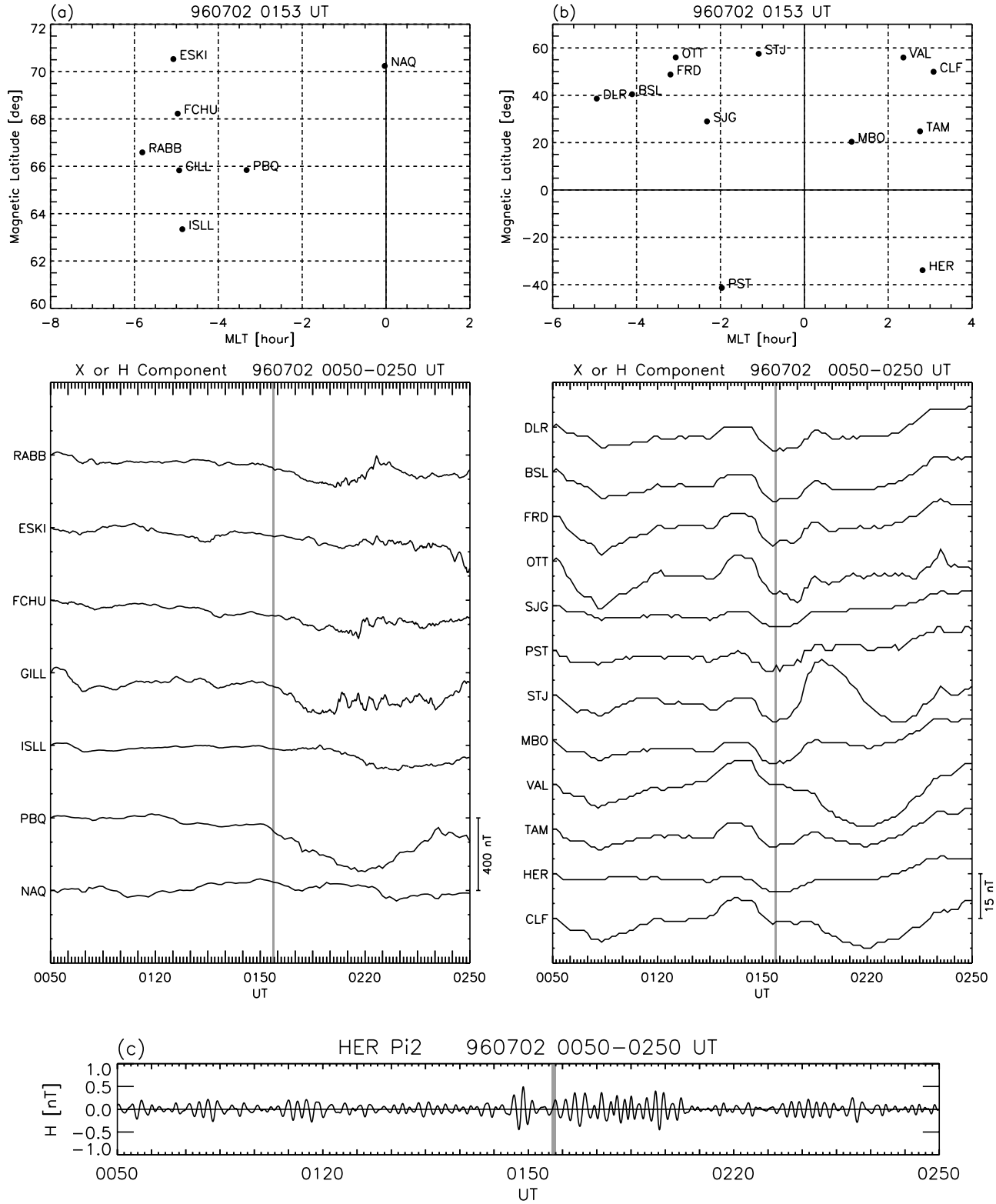


**Figure 3.** Locations of ground stations (a) at high latitudes, including selected CANOPUS stations (four-letter code), and (b) at low and middle latitudes, their north-south component of the geomagnetic field, and (c) the *H* component of Pi2 pulsations (40–150 s period) at Hermanus (HER) from 0050 to 0250 UT on 2 July 1996. The locations at the substorm expansion onset at 0153 UT are shown. The vertical lines indicate the substorm expansion onset determined from the Polar UVI data.

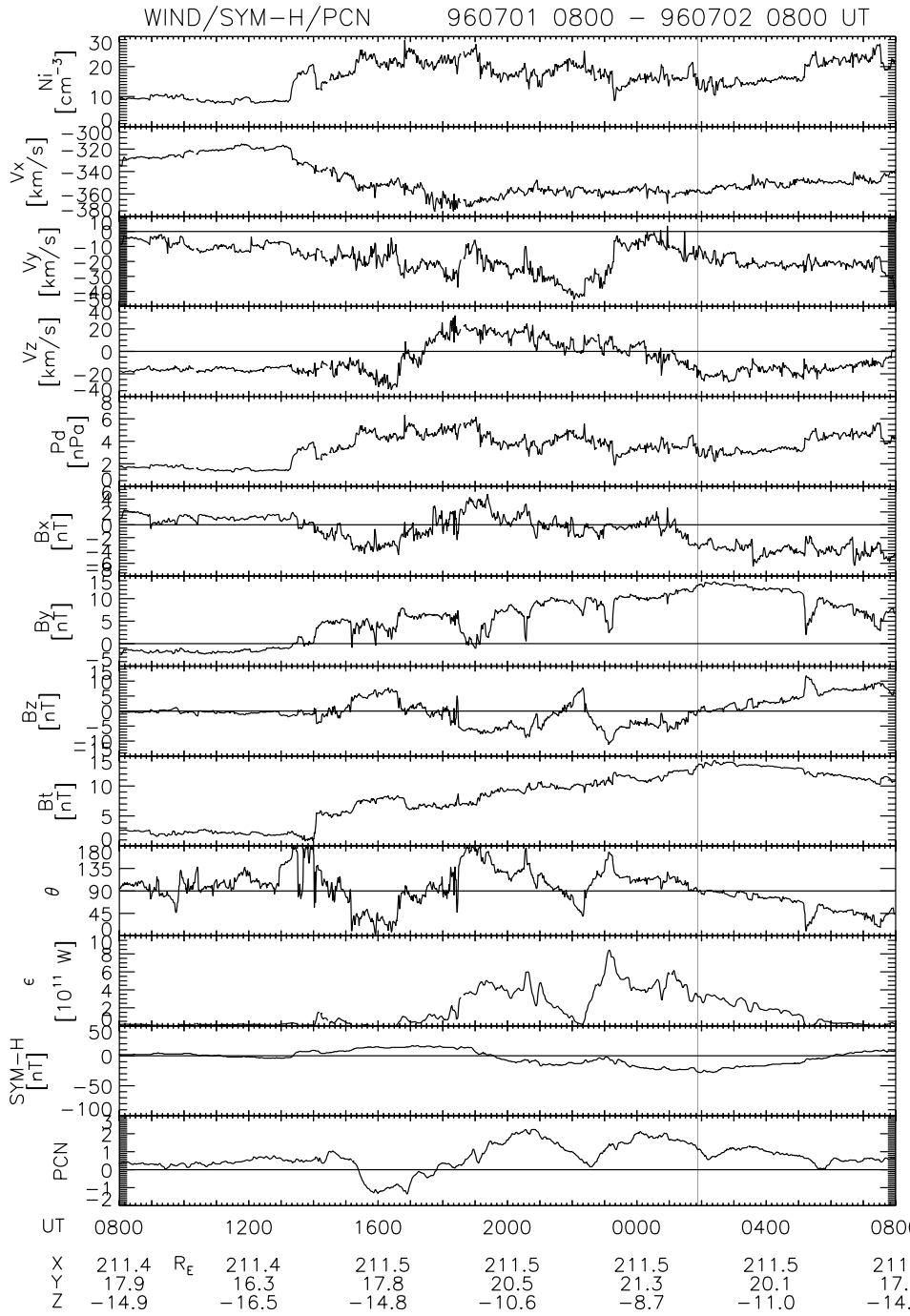


**Figure 4.** The solar wind parameters (the proton number density, the three components of the velocity, and the ion dynamic pressure), the interplanetary magnetic field (the three components, the total field, and the polar angle), and the epsilon parameter obtained by Wind in GSM coordinates, and the *SYM-H* and *PC* North indices from 0800 UT on 1 July 1996 to 0800 UT on 2 July 1996. The polar angle of the magnetic field 0°, 90°, and 180° correspond to the northward, dawn-dusk, and southward directions, respectively. The Wind data are shifted according to a propagation time from the Wind position to the dayside magnetopause, ∼62 min. The vertical line indicates the substorm expansion onset determined from the Polar UVI data.

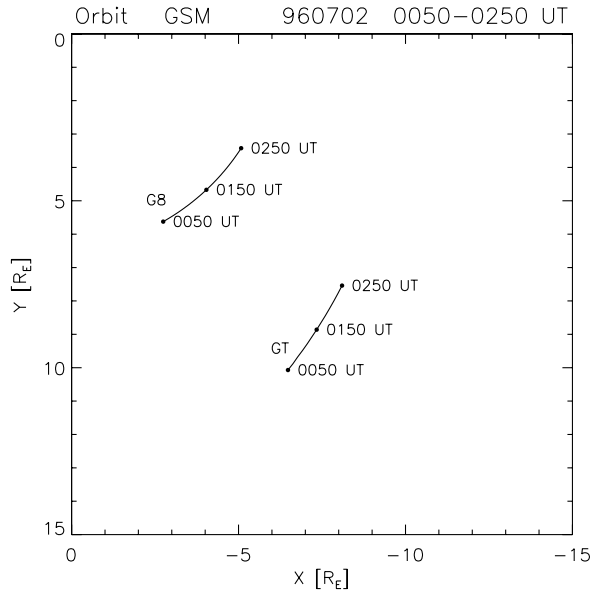


**Figure 5.** Locations of Geotail (GT) and GOES-8 (G8) in the GSM *X*-*Y* plane during the period from 0050 to 0250 UT on 2 July 1996.

sheet during ~0203–0206 UT. The total pressure, which is the sum of the ion and magnetic pressures, started to increase at ~0100 UT and then decreased ~1 min before the substorm expansion onset. Several southward excursions of $B_z$ were observed just before and after the onset. Then the dipolarization occurred at 0210 UT.

[13] Figure 7 shows expanded Geotail data for 0145–0205 UT. The northward $B_z$ decreased from ~0142 UT and became very small, ~0–2 nT, even in the central plasma sheet just before the onset. The Geotail location of $X \sim -7$ $R_E$ is usually near the inner edge of the tail or the transition region between the dipole-like and tail-like fields; the ambient magnetic field is dominated by the dipole field. The very small $B_z$ value in the present event, however, indicates that the magnetic field was much more stretched than usual. Just before and after the onset, a series of north-then-south bipolar $B_z$ and southward $B_z$ were observed: (1) ~0151:50–0153:05 UT, (2) ~0153:05–0154:20 UT, (3) ~0154:20–0155:20 UT, (4) ~0157:40–0200:10 UT, and (5) ~0200:20–0201:10 UT. Their durations were very short, ~1–2 min. The first two southward $B_z$ had clear prior enhancement of the northward $B_z$. According to the ion data and $B_x$, 1–3 were observed in the central plasma sheet, while 4–5 were observed away from the central plasma sheet. The duskward $B_y$ was very large during 1–3, possibly due to earthward field-aligned currents which existed northward of Geotail. The plasma flow $V_x$ was very stagnant for 1; it was tailward and perpendicular to the magnetic field but very slow, ~50–100 km/s, for 2 and 3, while it was tailward, parallel to the magnetic field, and faster, ~100–400 km/s, for 4 and 5. The last flow was observed near the auroral intensification at 0159 UT. All of 1–5 were accompanied by the enhancement of the perpendicular plasma flows toward the lobe. The total pressure and the total magnetic field enhanced near the southward turning of $B_z$, except for 2. As will be discussed later, these can be interpreted as signatures for plasmoids [cf., *Ieda et al.*, 1998], although they moved tailward very slowly. Their *X*-directional sizes were estimated to be ~0.5–3 $R_E$, based on their durations and flow speeds. The sizes were small and the durations were short compared to typical values in the middle and distant tail. These values obtained here are, however, comparable to typical values in the near-Earth tail [*Slavin et al.*, 2003, 2005]. (We checked the magnetic field data in SM coordinates to confirm that we can reach the same conclusions, since Geotail was located in the near-Earth region. The $B_z$ component was still clearly negative for 1–3. It became very small (nearly zero), however, for 4–5, so that 4–5 may possibly be different from plasmoids.)

[14] Figure 8 shows the energy-time spectrograms of electrons and ions obtained from the Geotail LEP energy analyzer for the same period as Figure 7. The upper part of the ion energy range was beyond the instrumental limit of ~40 keV/*q* during most of the period, which can result in an underestimate of the ion moments. A remarkable feature in the spectrograms is dawnward and duskward electrons with low energies of <~1 keV, observed near the central parts of the plasmoids for 1–4. An example of the distribution function for these low-energy bidirectional electrons is shown in Figure 9. The distribution function is two-dimensional, since there are unfortunately no three-dimensional distribution functions available for the period examined here. In addition to the isotropic component, highly collimated low-energy electrons were seen in the dawn-dusk direction or along the line between sectors 2–3 and 10–11. This direction was parallel to the magnetic field. *Frank et al.* [1994] as well as *Mukai et al.* [1996] reported the existence of such bidirectional field-aligned low-energy electrons in the vicinity of the central part of plasmoids. Taking into account the Geotail position, the strong duskward magnetic field, and the report that such electrons are also observed in the tail flanks [*Fujimoto et al.*, 1998], we infer that they originated from the magnetosheath.

[15] Figure 10 shows ion differential fluxes obtained from the ion composition subsystem of the Geotail energetic particles and ion composition instrument (EPIC-ICS) [*Williams et al.*, 1994] during 0145–0205 UT. Shown are energy-time spectrograms of ions with the energy range of 61.5–3005.4 keV (channels E3–E16) with 6, 48, or 96 s resolution, and azimuthal angular spectrograms and ratios between earthward and tailward fluxes and between duskward and dawnward fluxes for E3 (61.5–73.7 keV) and E5 (89.3–110.2 keV) channels with 6 and 48 s resolutions, respectively. It is seen that tailward fluxes were larger than earthward fluxes during the plasmoid observations and that duskward fluxes were larger than dawnward fluxes, as clearly shown by the flux ratios.

### 2.4. Geosynchronous Orbit

[16] The GOES-8 geosynchronous satellite was located in the premidnight sector at ($X$, $Y$) ~ (−4, 5) $R_E$, nearly radially aligned with Geotail: see Figure 5. The footprint of GOES-8 was at 65.1° (64.1°) AACGM latitude and 20.8 (20.9) hours MLT, ~1 hour eastward of the auroral onset region, according to the T89 (T96) model. Figure 11 shows magnetic field data obtained by GOES-8 with 0.512 s

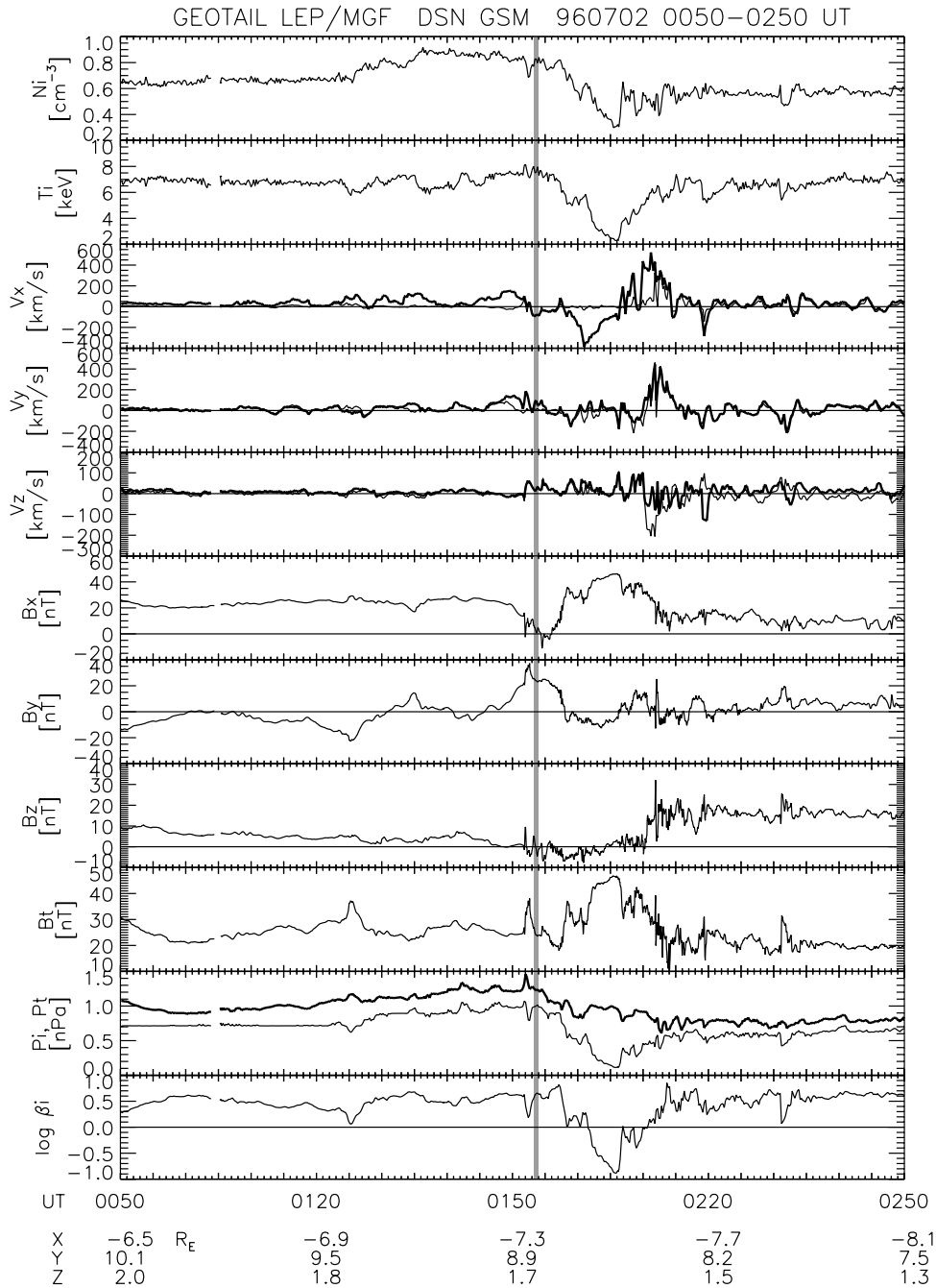


**Figure 6.** The ion number density, the ion temperature, the three components of the ion velocity (thick lines) and the ion velocity perpendicular to the magnetic field (thin lines), the three components of the magnetic field, the total magnetic field, the total (thick line) and ion (thin line) pressures, and the ion beta obtained by Geotail from 0050 to 0250 UT on 2 July 1996 in GSM coordinates. The vertical line indicates the substorm expansion onset determined from the Polar UVI data.

resolution. A clear dipolarization occurred at ~0156 UT, 2–3 min after the substorm onset, as indicated by an increase in the northward component and a decrease in the earthward component. The time delay is probably due to the eastward expansion of the auroral bulge to the GOES-8 position. Taking into account the increase in the westward component and the eastward expansion of the auroral bulge, it is most likely that GOES-8 was located earthward of the field-aligned current toward the ionosphere. Other dipolarizations occurred at 0202 and 0205 UT as well, corresponding to the auroral intensifications.

### 2.5. Ionospheric Convection

[17] We also examined ionospheric convection for this substorm event, using satellite and ground-based data. Figure 12 shows plasma bulk flows obtained from the Special Sensors-Ions, Electrons, and Scintillation (SSIES) on board the DMSP F12 and F13 satellites at an altitude of

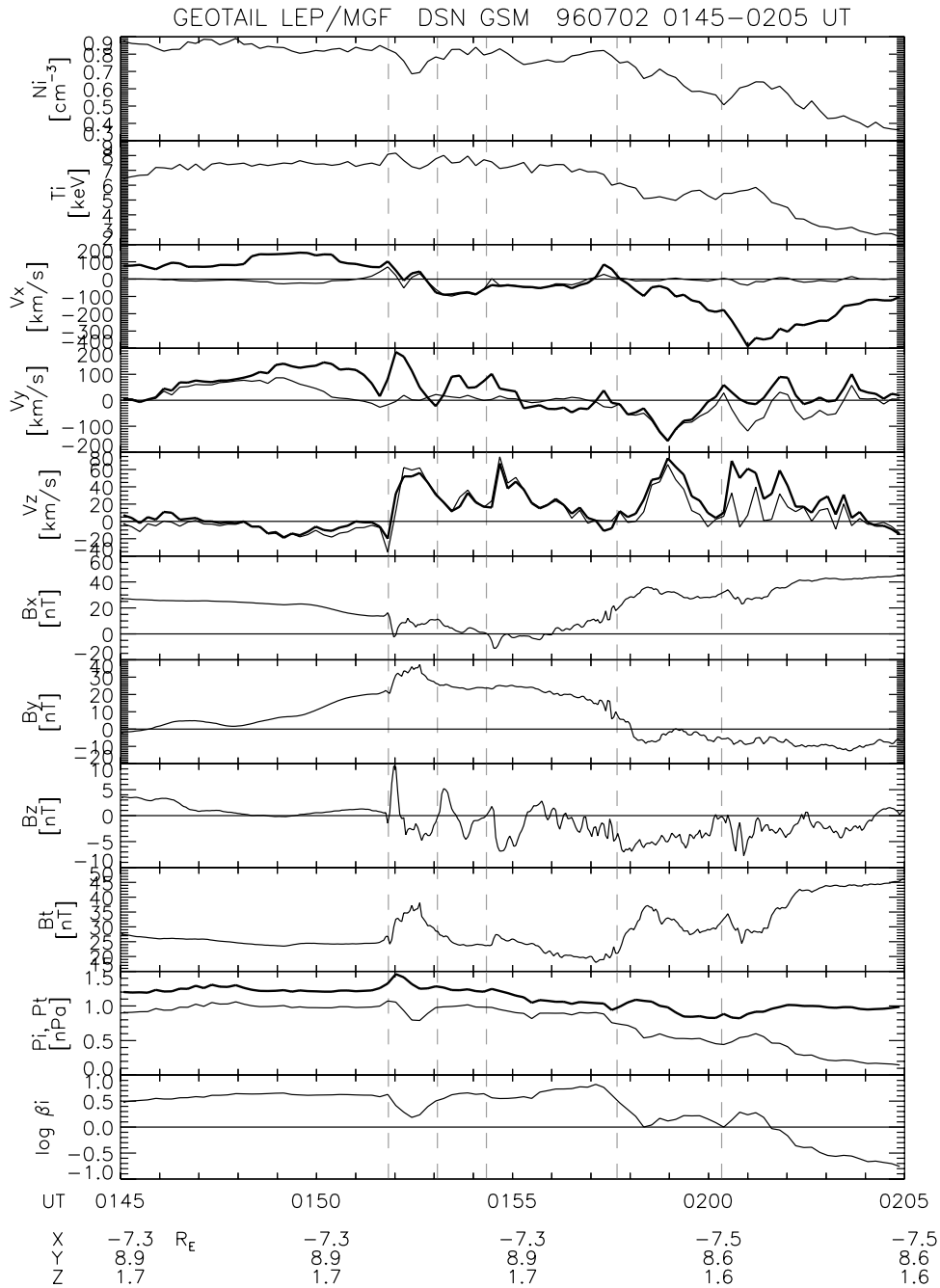


**Figure 7.** The ion moments and the magnetic field obtained by Geotail from 0145 to 0205 UT on 2 July 1996 in the same format as Figure 6. The vertical dashed lines indicate the start times of plasmoids.

~840 km in the northern hemisphere about 1 hour before the substorm onset, ~0040–0120 UT. While the flow speed was generally usual to somewhat strong, ~500–1000 m/s, the westward flows were stronger near the onset region at ~60°–70° and ~22 hours MLT, ~1500 m/s. The convection pattern is consistent with the convection model for the northern summer during IMF $B_z < 0$ and $B_y > 0$, i.e., the dusk cell became more dominant [*Papitashvili and Rich*, 2002].

[18] Super Dual Auroral Radar Network (SuperDARN) [*Greenwald et al.*, 1995] data near the auroral onset region were not available, but it is seen from Figure 13 that westward flows enhanced at ~70° in the midnight sector during 0158–0204 UT. During this enhancement, the midnight part of the auroral oval further expanded equatorward, reaching ~61°, and the auroral intensification occurred at 20–23 hours MLT, as shown in Figure 1.

## 3. Discussion

[19] For the 0153 UT substorm event on 2 July 1996, Geotail observed a series of tailward but slow flows with north-then-south magnetic fields fairly close to the Earth at $(X, Y) \sim (-7, 9)\ R_E$. Their $X$-directional sizes were

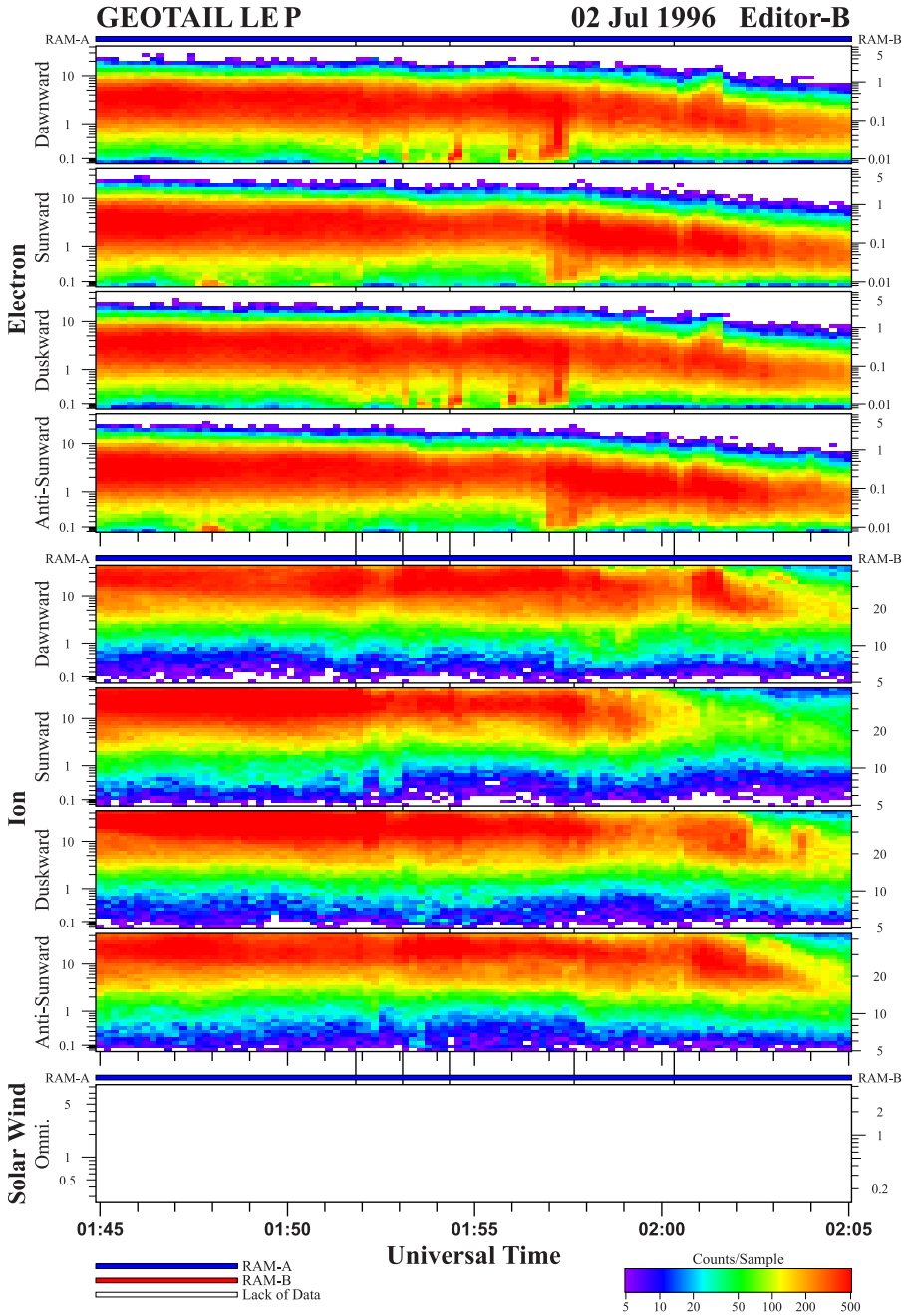


**Figure 8.** Energy-time spectrograms of (upper panels) electrons and (lower panels) ions obtained from the Geotail LEP energy analyzer from 0145 to 0205 UT on 2 July 1996. The vertical lines indicate the start times of plasmoids.

estimated to be $\sim$0.5–3 $R_E$, based on their durations and flow speeds. Possible scenarios for these observations are schematically illustrated in Figure 14: A multiple reconnection site, which is aligned in the $X$ direction, is formed to produce a series of tailward moving small plasmoids [*Finn and Kaw*, 1977; *Hoshino et al.*, 1994; *Slavin et al.*, 2003, 2005], or the magnetic reconnection successively occurs in various places, resulting in successive plasmoids [*Rastätter and Hesse*, 1999]. These plasmoids may then coalesce into larger plasmoids (Figure 14a). A single reconnection site is formed to produce a plasmoid and subsequent postplasmoid plasma sheet. Variable reconnection rates generate wavy structures in the north-south magnetic field [*Mukai et al.*, 1998] (Figure 14b). Some types of waves, such as kink-mode and sausage-mode waves, generate a series of north-south magnetic field variations [*Lee et al.*, 1988] (Figure 14c).

[20] Each of the observed structures was accompanied by an enhancement of the total pressure and the total magnetic field as well as the bidirectional field-aligned low-energy electrons in its central part. These features can often be seen near the central part of plasmoids [*Frank et al.*, 1994; *Mukai et al.*, 1996; *Ieda et al.*, 1998]. As pointed out by *Slavin et al.* [1989] and *Ieda et al.* [1998], enhancements of the

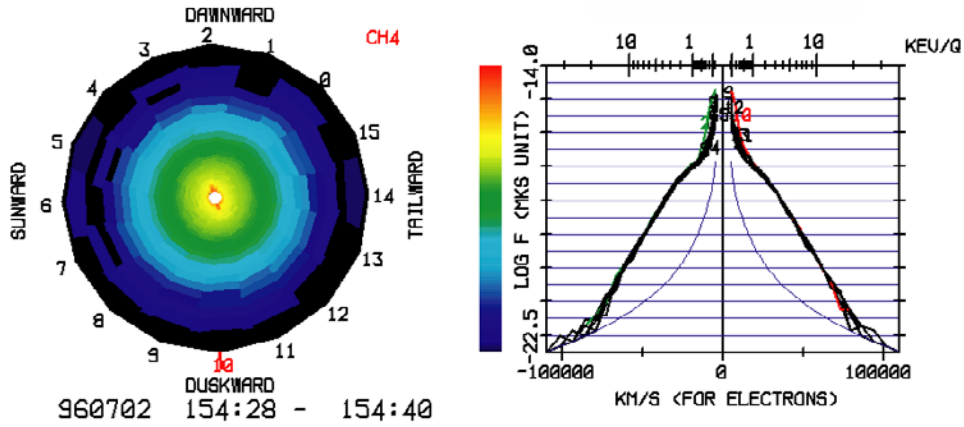


**Figure 9.** (left) Two-dimensional electron distribution function obtained from the Geotail LEP energy analyzer in a 12 s interval of 0154:28–0154:40 UT on 2 July 1996. (right) One-dimensional cuts of the electron distribution function for different sectors. The green and red lines indicate the distribution function for sectors 2 and 10, respectively.

total pressure and the total magnetic field cannot be seen in waves. Therefore we interpret the observed signatures as successive tailward moving small plasmoids, although they were much slower than usual plasmoids, i.e., quasi-stagnant plasmoids [*Nishida et al.*, 1986; *Kawano et al.*, 1996]. Slowly moving plasmoids at less than 200 km/s are sometimes observed in the near-Earth tail; see the examples of *Slavin et al.* [2003, 2005].

[21] Although the first plasmoid had an enhancement of $B_y$ and $B_t$ near its center, the latter four plasmoids were not

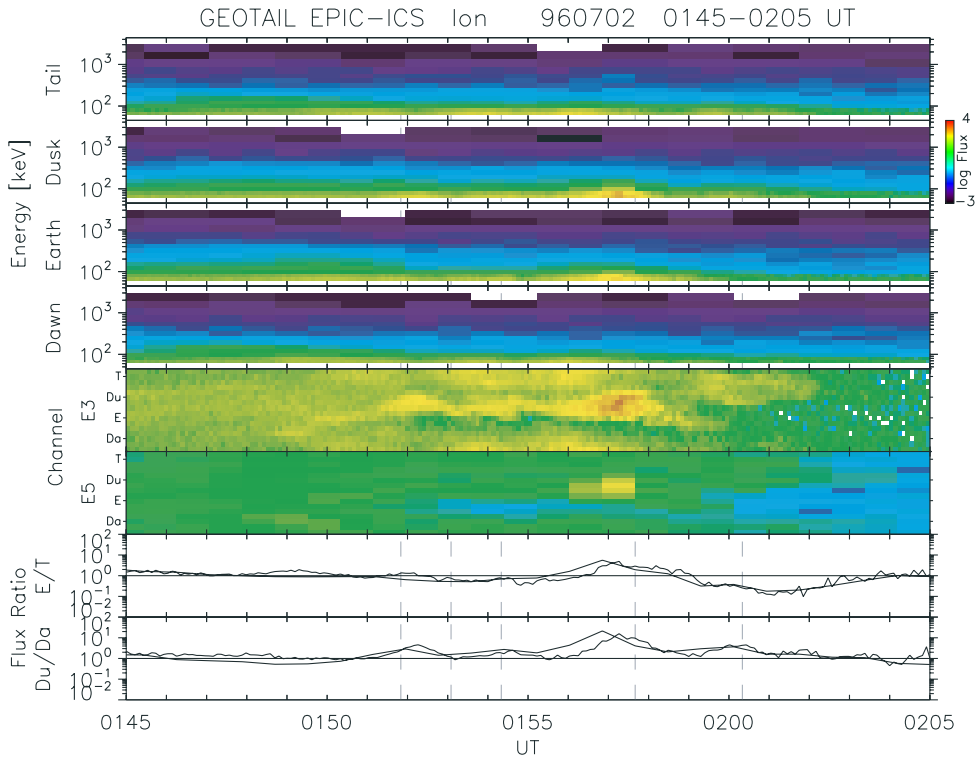


**Figure 10.** Ion differential fluxes obtained from the Geotail EPIC-ICS sensor from 0145 to 0205 UT on 2 July 1996 in $cm^{-2}\ s^{-1}\ sr^{-1}\ keV^{-1}$. Shown are energy-time spectrograms of ions with the energy range of 61.5–3005.4 keV (channels E3–E16) with 6, 48, or 96 s resolution, and azimuthal angular spectrograms and ratios between earthward and tailward fluxes and between duskward and dawnward fluxes for E3 (61.5–73.7 keV) and E5 (89.3–110.2 keV) channels with 6 and 48 s resolutions, respectively. T, Du, E, and Da of the azimuthal angular spectrograms and the panels of flux ratios denote tailward, duskward, earthward, and dawnward, respectively. The vertical dashed lines indicate the start times of plasmoids.

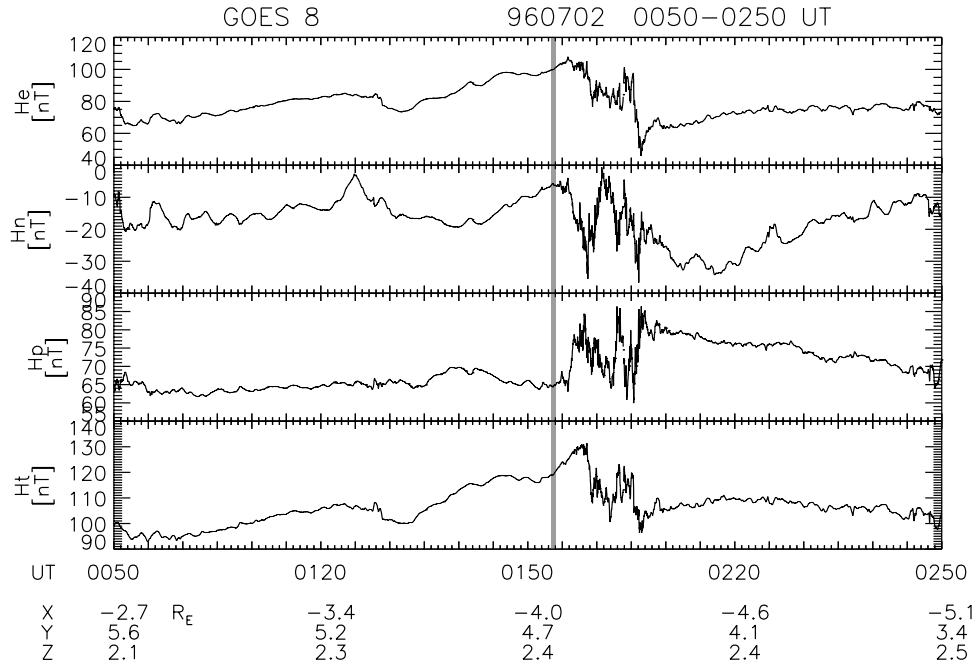


**Figure 11.** The earthward ($H_e$), eastward ($H_n$, normal to $H_p$ and $H_e$), and northward ($H_p$, perpendicular to the satellite orbit plane, or parallel to the Earth's rotation axis for a zero degree inclination orbit) components of the magnetic field and the total magnetic field ($H_t$) obtained by GOES-8 at geosynchronous orbit from 0050 to 0250 UT on 2 July 1996.

accompanied by significant $B_y$ enhancements. It is possible that the clear core $B_y$ field of the plasmoids did not develop very much soon after their formation [*Hesse et al.*, 1996a]. The last two plasmoids were observed away from the central plasma sheet so that the enhancement of $B_x$ and $B_t$ may be associated with the compression due to the central part of the plasmoids.

[22] The magnetic reconnection site ("NENL") at substorm expansion onset is located, on average, at $X \sim -20\,R_E$, but the magnetic reconnection site tends to be located closer to the Earth in more intense substorms [*Miyashita et al.*, 2004]. The magnetic reconnection is expected to occur very much close to the Earth, associated with a very intense substorm. However, considering that GOES-8 observed the dipolarization at $(X, Y) \sim (-4, 5)\ R_E$ after the onset, the magnetic reconnection must have occurred in $-4 > X > -7\,R_E$ for the 2 July 1996 substorm. This location is much closer to the Earth than usual, although the intensity of this substorm was moderate. Our interpretation is different from that of *Frank et al.* [2001], who examined the same substorm event that we examined in the present paper and suggested that a series of bursts of the southward $B_z$ discussed in the present paper was produced by magnetic reconnection, but it was not related to the "NENL."

[23] The tailward flows with the southward $B_z$ were observed until ~0207 UT. Then the flows turned earthward, and the northward $B_z$ increased at ~0210 UT, in conjunction with the dipolarization. These observations suggest that the magnetic reconnection site remained earthward of Geotail until ~0207 UT and then retreated tailward. Also, while the first four plasmoids were very stagnant, the last plasmoid was fast, which was observed near the auroral intensification at 0159 UT. It is possible that the last plasmoid swept away the former plasmoids along down the tail.

[24] Plasmoids almost always correspond to auroral breakups including pseudobreakups [*Ieda et al.*, 2001]. It seems, however, that for the 2 July 1996 substorm, only the plasmoids at 0152 and 0200 UT correspond to the auroral breakup and intensification, respectively, whereas the other

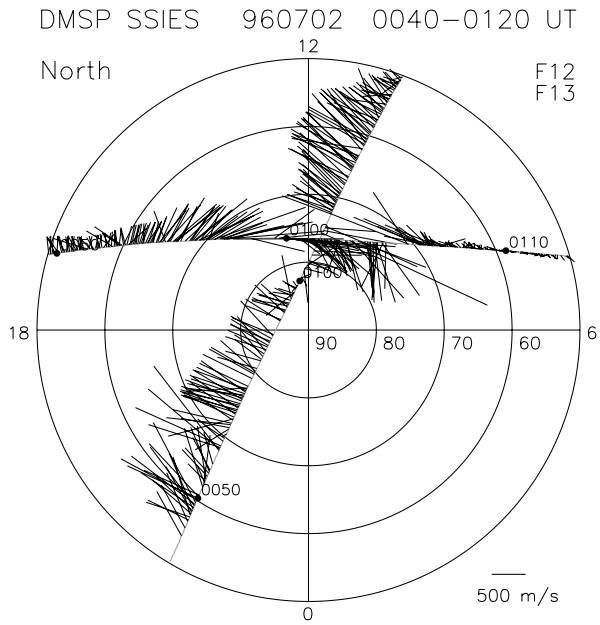


**Figure 12.** Plasma bulk flows obtained from DMSP F12 and F13 SSIES at an altitude of ~840 km in the northern hemisphere about 1 hour before the substorm onset, ~0040–0120 UT. F12 and F13 are in 2200–1030 local time and dusk-dawn orientations, respectively.

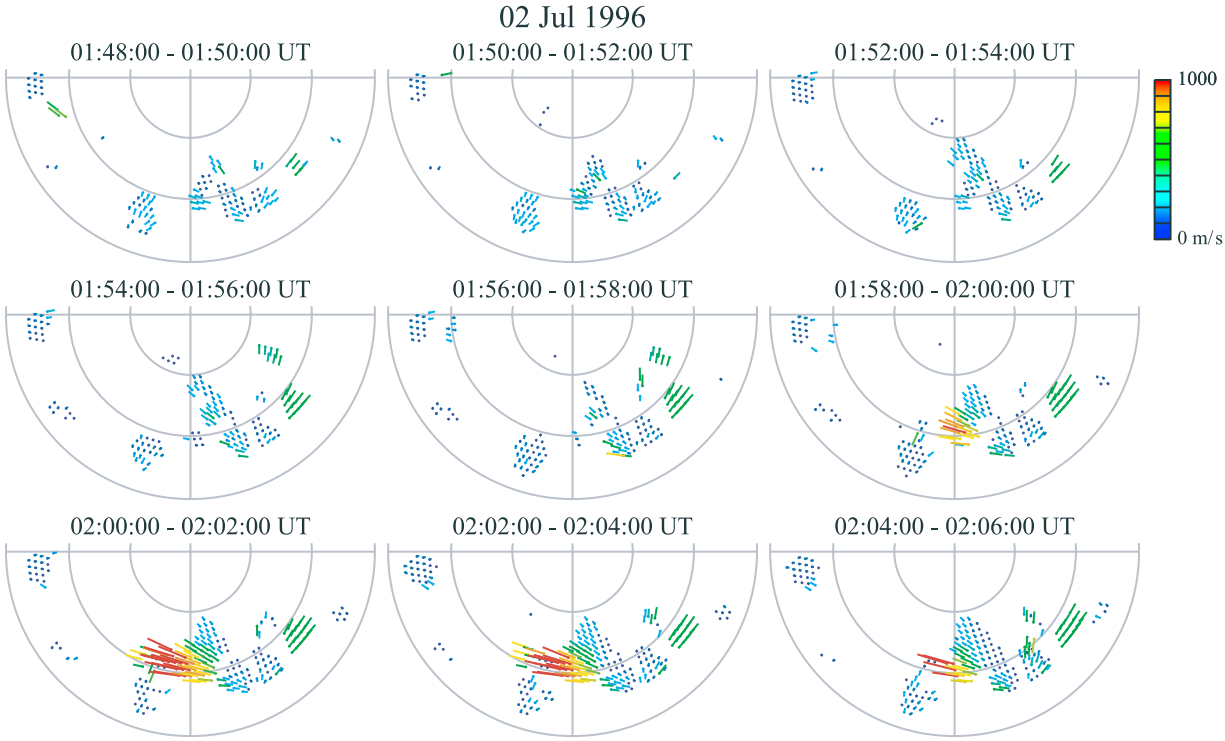


**Figure 13.** Nightside ionospheric line-of-sight velocities measured by SuperDARN radars at Saskatoon, Kapuskasing, Goose Bay, Stokkseyri, Pikkvibaer, and Hankasalmi in the northern hemisphere for 2-min intervals from 0148 to 0206 UT. The magnetic midnight and dusk are plotted to the bottom and left, respectively. The contours of magnetic latitudes are drawn from 90° with a decrement of 10°.

plasmoids were not accompanied by any clear auroral signatures. It is possible that only the dominant magnetic reconnection affects the dipolarization and the field-aligned currents earthward of the magnetic reconnection sites, even if the magnetic reconnection occurs in more than one region [*Rastätter and Hesse*, 1999].

[25] It is known that the convection plays an important role in the formation of the thin current sheet in the magnetotail [*Pritchett and Coroniti*, 1994; *Cai et al.*, 1995; *Hesse et al.*, 1996b; *Tanaka*, 2000]. *Pritchett and Coroniti* [2001] showed that a localized convection results in a localized thin current sheet and thus magnetic reconnection. *Kan and Sun* [1996] proposed that a localized strong convection is required for the substorm expansion phase to take place in addition to the global convection. It is reported that the ionospheric flow speed enhances near the auroral breakup region around substorm expansion onset [*Lester*, 2000; *Bristow et al.*, 2001; *Liang et al.*, 2004; *Provan et al.*, 2004]. For the 2 July 1996 substorm, the polar cap magnetic activity index (*PC* north) [*Troshichev et al.*, 1988] started to decrease just before the onset, from ~1.4 at ~0148 UT to ~0.6 at 0212 UT, as shown in the bottom panel of Figure 4. These values correspond to cross polar cap potentials of 36 and 20 kV and polar cap diameters of 31° and 27°, respectively [*Troshichev et al.*, 1996]. These cross polar cap potentials were not very large, indicating that the global ionospheric convection was not very strong around the onset. The DMSP SSIES and SuperDARN data, however, show that the ionospheric convection was locally enhanced near the onset region, although the enhancement was observed about 1 hour before the onset and ~5 min after the onset, respectively. As shown by the Polar UVI observations, the latitude of the auroral oval was ~10° lower than what was estimated from the *PC* index. Hence we surmise that the convection was highly enhanced locally near the onset region, leading to the formation of the thin current sheet and the magnetic reconnection and producing the plasmoids much closer to the Earth than usual.

[26] The locally enhanced convection in the dusk sector might be caused by the effect of the large IMF $B_y$ [cf.,

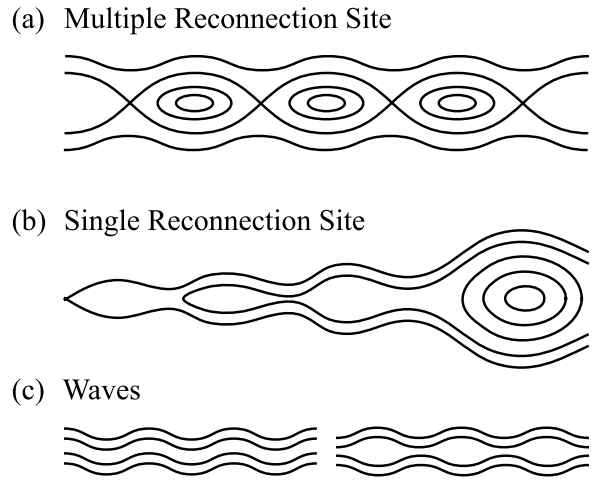


**Figure 14.** Two-dimensional schematics of possible scenarios for a series of tailward flows with north-then-south magnetic fields observed by Geotail.

*Kozlovsky et al.*, 2003]. In fact, the Wind data show that before the onset of the 2 July 1996 substorm, the large duskward IMF $B_y$ lasted for more than 12 hours, while the southward IMF $B_z$ was not very large. It is also plausible that the somewhat large solar wind dynamic pressure may cause the expansion of the auroral oval [*Kabin et al.*, 2004], leading to the substorm onset at lower latitudes [*Gérard et al.*, 2004].

[27] **Acknowledgments.** The Geotail MGF magnetic field data were provided by S. Kokubun and T. Nagai. The geomagnetic field data and the *SYM-H* and *Dst* indices were provided by World Data Center for Geomagnetism, Kyoto. The *Kp* index was provided by GeoForschungsZentrum Potsdam. The *PC* index was provided by World Data Center for Geomagnetism, Copenhagen, and World Data Center for Solar Terrestrial Physics, Moscow. The CANOPUS instrument array, constructed, maintained, and operated by the Canadian Space Agency, provided the geomagnetic field data used in this study. We thank F. Creutzberg for the CANOPUS data. The geomagnetic field data obtained at Hermanus were provided by P. R. Sutcliffe. The Wind SWE plasma data and the Wind MFI magnetic field data were provided by K. Ogilvie and R. Lepping, respectively, through the Coordinated Data Analysis Web (CDAWeb) at NASA. The hourly values of the solar wind and IMF (OMNI 2 data) were provided by National Space Science Data Center at NASA. The GOES magnetic field data were provided by H. J. Singer. The DMSP SSIES thermal plasma data were provided by the Center for Space Sciences at the University of Texas at Dallas and the U.S. Air Force. The SuperDARN data obtained at Kapuskasing and Goose Bay were provided by R. A. Greenwald. We thank all the staffs who contributed to the operation of the SuperDARN radars. We also thank M. Nosé and K. Keika for their help in preparing Geotail EPIC data and H. J. Singer, M. Nosé, K. S. Park, and Y. Miyoshi for their useful comments. One of the authors (Y.M.) was supported by Research Fellowships of the Japan Society for the Promotion of Science for Young Scientists.

[28] Lou-Chuang Lee thanks Vassilis Angelopoulos and another reviewer for their assistance in evaluating this paper.

## References

Agelopoulos, V., et al. (1996), Tailward propagation of magnetotail acceleration centers: Relationship to substorm current wedge, *J. Geophys. Res.*, *101*, 24,599–24,619.

Baker, D. N., T. I. Pulkkinen, V. Angelopoulos, W. Baumjohann, and R. L. McPherron (1996), Neutral line model of substorms: Past results and present view, *J. Geophys. Res.*, *101*, 12,975–13,010.

Baker, K. B., and S. Wing (1989), A new magnetic coordinate system for conjugate studies at high latitudes, *J. Geophys. Res.*, *94*, 9139–9143.

Baumjohann, W., G. Paschmann, and C. A. Cattell (1989), Average plasma properties in the central plasma sheet, *J. Geophys. Res.*, *94*, 6597–6606.

Baumjohann, W., M. Hesse, S. Kokubun, T. Mukai, T. Nagai, and A. A. Petrukovich (1999), Substorm dipolarization and recovery, *J. Geophys. Res.*, *104*, 24,995–25,000.

Bristow, W. A., A. Otto, and D. Lummerzheim (2001), Substorm convection patterns observed by the Super Dual Auroral Radar Network, *J. Geophys. Res.*, *106*, 24,593–24,609.

Cai, H. J., L. C. Lee, and L. Zhang (1995), Tailward stretching of geomagnetic field lines in the presence of an enhanced ionospheric convection electric field, *Geophys. Res. Lett.*, *22*, 3449–3452.

Craven, J. D., and L. A. Frank (1991), Diagnosis of auroral dynamics using global auroral imaging with emphasis on large-scale evolutions, in *Auroral Physics*, edited by C.-I. Meng, M. J. Rycroft, and L. A. Frank, pp. 273–288, Cambridge Univ. Press, New York.

Finn, J. M., and P. K. Kaw (1977), Coalescence instability of magnetic islands, *Phys. Fluids*, *20*, 72–78.

Forbes, T. G., E. W. Hones, S. J. Bame, J. R. Asbridge, G. Paschmann, N. Sckopke, and C. T. Russell (1981), Evidence for the tailward retreat of a magnetic neutral line in the magnetotail during substorm recovery, *Geophys. Res. Lett.*, *8*, 261–264.

Frank, L. A., W. R. Paterson, K. L. Ackerson, S. Kokubun, T. Yamamoto, D. H. Fairfield, and R. P. Lepping (1994), Observations of plasmas associated with the magnetic signature of a plasmoid in the distant magnetotail, *Geophys. Res. Lett.*, *21*, 2967–2970.

Frank, L. A., J. B. Sigwarth, W. R. Paterson, and S. Kokubun (2001), Two encounters of the substorm onset region with the Geotail spacecraft, *J. Geophys. Res.*, *106*, 5811–5831.

Fujimoto, M., T. Terasawa, T. Mukai, Y. Saito, T. Yamamoto, and S. Kokubun (1998), Plasma entry from the flanks of the near-Earth magnetotail: Geotail observations, *J. Geophys. Res.*, *103*, 4391–4408.

Gérard, J.-C., B. Hubert, A. Grard, M. Meurant, and S. B. Mende (2004), Solar wind control of auroral substorm onset locations observed with the IMAGE-FUV imagers, *J. Geophys. Res.*, *109*, A03208, doi:10.1029/2003JA010129.

Greenwald, R. A., et al. (1995), DARN/SuperDARN: A global view of the dynamics of high-latitude convection, *Space Sci. Rev.*, *71*, 761–796.

Hesse, M., J. Birn, M. M. Kuznetsova, and J. Dreher (1996a), A simple model of core field generation during plasmoid evolution, *J. Geophys. Res.*, *101*, 10,797–10,804.

Hesse, M., D. Winske, M. Kuznetsova, J. Birn, and K. Schindler (1996b), Hybrid modeling of the formation of thin current sheets in magnetotail configurations, *J. Geomagn. Geoelectr.*, *48*, 749–763.

Hones, H. W., Jr. (1976), The magnetotail: Its generation and dissipation, in *Physics of Solar Planetary Environments*, edited by D. J. Williams, pp. 558–571, AGU, Washington, D. C.

Hoshino, M., A. Nishida, T. Yamamoto, and S. Kokubun (1994), Turbulent magnetic field in the distant magnetotail: Bottom-up process of plasmoid formation?, *Geophys. Res. Lett.*, *21*, 2935–2938.

Ieda, A., S. Machida, T. Mukai, Y. Saito, T. Yamamoto, A. Nishida, T. Terasawa, and S. Kokubun (1998), Statistical analysis of the plasmoid evolution with Geotail observations, *J. Geophys. Res.*, *103*, 4453–4465.

Ieda, A., D. H. Fairfield, T. Mukai, Y. Saito, S. Kokubun, K. Liou, C.-I. Meng, G. K. Parks, and M. J. Brittnacher (2001), Plasmoid ejection and auroral brightenings, *J. Geophys. Res.*, *106*, 3845–3857.

Kabin, K., R. Rankin, G. Rostoker, R. Marchand, I. J. Rae, A. J. Ridley, T. I. Gombosi, C. R. Clauer, and D. L. DeZeeuw (2004), Open-closed field line boundary position: A parametric study using an MHD model, *J. Geophys. Res.*, *109*, A05222, doi:10.1029/2003JA010168.

Kadokura, A., A. Yukimatu, M. Ejiri, T. Oguti, M. Pinnock, and P. R. Sutcliffe (2002), Detailed analysis of a substorm event on 6 and 7 June 1989: 2. Stepwise auroral bulge evolution during expansion phase, *J. Geophys. Res.*, *107*(A12), 1480, doi:10.1029/2001JA009129.

Kan, J. R., and W. Sun (1996), Substorm expansion phase caused by an intense localized convection imposed on the ionosphere, *J. Geophys. Res.*, *101*, 27,271–27,281.

Kawano, H., et al. (1996), A quasi-stagnant plasmoid observed with Geotail on October 15, 1993, *J. Geomagn. Geoelectr.*, *48*, 525–539.

Kokubun, S., T. Yamamoto, M. H. Acuña, K. Hayashi, K. Shiokawa, and H. Kawano (1994), The GEOTAIL magnetic field experiment, *J. Geomagn. Geoelectr.*, *46*, 7–21.

Kozlovsky, A., T. Turunen, A. Koustov, and G. Parks (2003), IMF By effects in the magnetospheric convection on closed magnetic field lines, *Geophys. Res. Lett.*, *30*(24), 2261, doi:10.1029/2003GL018457.

Lee, L. C., S. Wang, C. Q. Wei, and B. T. Tsurutani (1988), Streaming sausage, kink and tearing instabilities in a current sheet with applications to the Earth's magnetotail, *J. Geophys. Res.*, *93*, 7354–7365.

Lester, M. (2000), HF coherent scatter radar observations of ionospheric convection during magnetospheric substorms, *Adv. Polar Upper Atmos. Res.*, *14*, 179–201.

Liang, J., G. J. Sofko, E. F. Donovan, M. Watanabe, and R. A. Greenwald (2004), Convection dynamics and driving mechanism of a small substorm during dominantly IMF By+, Bz+ conditions, *Geophys. Res. Lett.*, *31*, L08803, doi:10.1029/2003GL018878.

Liou, K., P. T. Newell, D. G. Sibeck, C.-I. Meng, M. Brittnacher, and G. Parks (2001), Observation of IMF and seasonal effects in the location of auroral substorm onset, *J. Geophys. Res.*, *106*, 5799–5810.

Lui, A. T. Y. (1996), Current disruption in the Earth's magnetosphere: Observations and models, *J. Geophys. Res.*, *101*, 13,067–13,088.

Machida, S., Y. Miyashita, A. Ieda, A. Nishida, T. Mukai, Y. Saito, and S. Kokubun (1999), GEOTAIL observations of flow velocity and north-south magnetic field variations in the near and mid-distant tail associated with substorm onsets, *Geophys. Res. Lett.*, *26*, 635–638.

Miyashita, Y., S. Machida, T. Mukai, Y. Saito, K. Tsuruda, H. Hayakawa, and P. R. Sutcliffe (2000), A statistical study of variations in the near and middistant magnetotail associated with substorm onsets: GEOTAIL observations, *J. Geophys. Res.*, *105*, 15,913–15,930.

Miyashita, Y., S. Machida, K. Liou, T. Mukai, Y. Saito, H. Hayakawa, C.-I. Meng, and G. K. Parks (2003), Evolution of the magnetotail associated with substorm auroral breakups, *J. Geophys. Res.*, *108*(A9), 1353, doi:10.1029/2003JA009939.

Miyashita, Y., Y. Kamide, S. Machida, K. Liou, T. Mukai, Y. Saito, A. Ieda, C.-I. Meng, and G. K. Parks (2004), Difference in magnetotail variations between intense and weak substorms, *J. Geophys. Res.*, *109*, A11205, doi:10.1029/2004JA010588.

Miyashita, Y., et al. (2005), Geotail observations of signatures in the near-Earth magnetotail for the extremely intense substorms of the 30 October 2003 storm, *J. Geophys. Res.*, *110*, A09S25, doi:10.1029/2005JA011070.

Mukai, T., S. Machida, Y. Saito, M. Hirahara, T. Terasawa, N. Kaya, T. Obara, M. Ejiri, and A. Nishida (1994), The low energy particle

(LEP) experiment onboard the GEOTAIL satellite, *J. Geomagn. Geoelectr.*, *46*, 669–692.

Mukai, T., M. Fujimoto, M. Hoshino, S. Kokubun, S. Machida, K. Maezawa, A. Nishida, Y. Saito, T. Terasawa, and T. Yamamoto (1996), Structure and kinetic properties of plasmoids and their boundary regions, *J. Geomagn. Geoelectr.*, *48*, 541–560.

Mukai, T., T. Yamamoto, and S. Machida (1998), Dynamics and kinetic properties of plasmoids and flux ropes: GEOTAIL observations, in *New Perspectives on the Earth's Magnetotail*, edited by A. Nishida, D. N. Baker, and S. W. H. Cowley, pp. 117–137, AGU, Washington, D. C.

Nagai, T., M. Fujimoto, Y. Saito, S. Machida, T. Terasawa, R. Nakamura, T. Yamamoto, T. Mukai, A. Nishida, and S. Kokubun (1998), Structure and dynamics of magnetic reconnection for substorm onsets with Geotail observations, *J. Geophys. Res.*, *103*, 4419–4440.

Nishida, A., M. Scholer, T. Terasawa, S. J. Bame, G. Gloeckler, E. J. Smith, and R. D. Zwickl (1986), Quasi-stagnant plasmoid in the middle tail: A new preexpansion phase phenomenon, *J. Geophys. Res.*, *91*, 4245–4255.

Papitashvili, V. O., and F. J. Rich (2002), High-latitude ionospheric convection models derived from Defense Meteorological Satellite Program ion drift observations and parameterized by the interplanetary magnetic field strength and direction, *J. Geophys. Res.*, *107*(A8), 1198, doi:10.1029/2001JA000264.

Pritchett, P. L., and F. V. Coroniti (1994), Convection and the formation of thin current sheets in the near-Earth plasma sheet, *Geophys. Res. Lett.*, *21*, 1587–1590.

Pritchett, P. L., and F. V. Coroniti (2001), Kinetic simulations of 3-D reconnection and magnetotail disruptions, *Earth Planets Space*, *53*, 635–643.

Provan, G., M. Lester, S. B. Mende, and S. E. Milan (2004), Statistical study of high-latitude plasma flow during magnetospheric substorms, *Ann. Geophys.*, *22*, 3607–3624.

Rastätter, L., and M. Hesse (1999), Patchy reconnection and evolution of multiple plasmoids in the Earth's magnetotail: Effects on near-Earth current system, *J. Geophys. Res.*, *104*, 25,011–25,020.

Rostoker, G., J. C. Samson, F. Creutzberg, T. J. Hughes, D. R. McDiarmid, A. G. McNamara, A. Vallance Jones, D. D. Wallis, and L. L. Cogger (1995), CANOPUS-A ground-based instrument array for remote sensing the high latitude ionosphere during the ISTP/GGS program, *Space Sci. Rev.*, *71*, 743–760.

Slavin, J. A., et al. (1989), CDAW 8 observations of plasmoid signatures in the geomagnetic tail: An assessment, *J. Geophys. Res.*, *94*, 15,153–15,175.

Slavin, J. A., R. P. Lepping, J. Gjerloev, D. H. Fairfield, M. Hesse, C. J. Owen, M. B. Moldwin, T. Nagai, A. Ieda, and T. Mukai (2003), Geotail observations of magnetic flux ropes in the plasma sheet, *J. Geophys. Res.*, *108*(A1), 1015, doi:10.1029/2002JA009557.

Slavin, J. A., E. I. Tanskanen, M. Hesse, C. J. Owen, M. W. Dunlop, S. Imber, E. A. Lucek, A. Balogh, and K.-H. Glassmeier (2005), Cluster observations of traveling compression regions in the near-tail, *J. Geophys. Res.*, *110*, A06207, doi:10.1029/2004JA010878.

Tanaka, T. (2000), The state transition model of the substorm onset, *J. Geophys. Res.*, *105*, 21,081–21,096.

Torr, M. R., et al. (1995), A far ultraviolet imager for the international solar-terrestrial physics mission, *Space Sci. Rev.*, *71*, 329–383.

Troshichev, O. A., V. G. Andrezen, S. Vennerstrøm, and E. Friis-Christensen (1988), Magnetic activity in the polar cap—A new index, *Planet. Space Sci.*, *36*, 1095–1102.

Troshichev, O. A., H. Hayakawa, A. Matsuoka, T. Mukai, and K. Tsuruda (1996), Cross polar cap diameter and voltage as a function of *PC* index and interplanetary quantities, *J. Geophys. Res.*, *101*, 13,429–13,435.

Tsyganenko, N. A. (1989), A magnetospheric magnetic field model with a warped tail current sheet, *Planet. Space Sci.*, *37*, 5–20.

Tsyganenko, N. A. (1995), Modeling the Earth's magnetospheric magnetic field confined within a realistic magnetopause, *J. Geophys. Res.*, *100*, 5599–5612.

Ueno, G., S. Machida, T. Mukai, Y. Saito, and A. Nishida (1999), Distribution of X-type magnetic neutral lines in the magnetotail with Geotail observations, *Geophys. Res. Lett.*, *26*, 3341–3344.

Williams, D. J., R. W. McEntire, C. Schlemm II, A. T. Y. Lui, G. Gloeckler, S. P. Christon, and F. Gliem (1994), GEOTAIL energetic particles and ion composition instrument, *J. Geomagn. Geoelectr.*, *46*, 39–57.

A. Ieda, Y. Kamide, Y. Miyashita, and N. Nishitani, Solar-Terrestrial Environment Laboratory, Nagoya University, Toyokawa, Aichi 442-8507, Japan. (ieda@stelab.nagoya-u.ac.jp; kamide@stelab.nagoya-u.ac.jp; miyasita@stelab.nagoya-u.ac.jp; nisitani@stelab.nagoya-u.ac.jp)

M. Lester, Department of Physics and Astronomy, University of Leicester, Leicester, LE1 7RH, UK. (mle@ion.le.ac.uk)

K. Liou, R. W. McEntire, and C.-I. Meng, Johns Hopkins University Applied Physics Laboratory, Laurel, MD 20723, USA. (kan.liou@jhuapl.edu; richard.mcentire@jhuapl.edu; ching.meng@jhuapl.edu)

S. Machida, Department of Geophysics, Kyoto University, Kyoto 606-8502, Japan. (machida@kugi.kyoto-u.ac.jp)

T. Mukai and Y. Saito, Institute of Space and Astronautical Science, Japan Aerospace Exploration Agency, Sagamihara, Kanagawa 229-8510, Japan. (mukai@stp.isas.jaxa.jp; saito@stp.isas.jaxa.jp)

G. K. Parks, Space Sciences Laboratory, University of California, Berkeley, Berkeley, CA 94720, USA. (parks@ssl.berkeley.edu)

G. J. Sofko, Institute of Space and Atmospheric Studies, University of Saskatchewan, Saskatoon, SKS7N 5E2, Canada. (george. sofko@usask.ca)

J.-P. Villain, Laboratoire de Physique et Chimie de l'Environnement, Centre National de la Recherche Scientifique, 45071 Orléans, Cedex 2, France. (jvillain@cnrs-orleans.fr)